

Light-addressable liquid crystal polymer dispersed liquid crystal

LUCIANO DE SIO,^{1,*} ELENA OUSKOVA,¹ PAMELA LLOYD,² RAFAEL VERGARA,¹ NELSON TABIRYAN,¹ AND TIMOTHY J. BUNNING²

¹Beam Engineering for Advanced Measurements Co. (BEAM Co.), 1300 Lee Rd, Orlando, FL 32810, USA

²Air Force Research Laboratory, Wright-Patterson Air Force Base, OH 45433-7707, USA

*info@beamco.com

Abstract: Scattering-free liquid crystal polymer-dispersed liquid crystal polymer (LCPDLC) films are fabricated by combining a room temperature polymerizable liquid crystal (LC) monomer with a mesogenic photosensitive LC. The morphological and photosensitive properties of the system are analysed with polarized optical microscopy and high resolution scanning and transmission electron microscopy. A two-phase morphology comprised of oriented fibril-like polymeric structures interwoven with nanoscale domains of phase separated LC exists. The nanoscale of the structures enables an absence of scattering which allows imaging through the LCPDLC sample without optical distortion. The use of a mesogenic monomer enables much smaller phase separated domains as compared to non-mesogenic systems. All-optical experiments show that the transmitted intensity, measured through parallel polarizers, can be modulated by the low power density radiation (31 mW/cm²) of a suitable wavelength (532 nm). The reversible and repeatable transmission change is due to the photoinduced *trans-cis* photoisomerization process. The birefringence variation (0.01) obtained by optically pumping the LCPDLC films allow their use as an all-optical phase modulator.

© 2017 Optical Society of America

OCIS codes: (230.0230) Optical devices; (230.1150) All-optical devices; (230.3720) Liquid-crystal devices; (160.3710) Liquid crystals; (160.5335) Photosensitive materials; (160.4670) Optical materials.

References and links

1. T. Ikeda and O. Tsutsumi, "Optical switching and image storage by means of azobenzene liquid-crystal films," *Science* **268**(5219), 1873–1875 (1995).
2. M. C. Gupta, *Handbook of Photonics* (CRC Press, 1997).
3. I. C. Khoo, "Nonlinear optics of liquid crystalline materials," *Phys. Rep.* **471**(5-6), 221–267 (2009).
4. H. K. Lee, A. Kanazawa, T. Shiono, T. Ikeda, T. Fujisawa, M. Aizawa, and B. Lee, "All-optically controllable polymer/liquid crystal composite films containing the azobenzene liquid crystal," *Chem. Mater.* **10**(5), 1402–1407 (1998).
5. A. Shishido, A. Kanazawa, T. Shiono, T. Ikeda, and N. Tamai, "Enhancement of stability in optical switching of photosensitive liquid crystal by means of reflection mode analysis," *J. Mater. Chem.* **9**(9), 2211–2213 (1999).
6. I. C. Khoo, P. H. Chen, M. Y. Shih, A. Shishido, S. Slussarenko, and M. V. Wood, "Supra optical nonlinearities (SON) of methyl red- and azobenzene liquid crystal - doped nematic liquid crystals," *Mol. Cryst. Liq. Cryst. (Phila. Pa.)* **358**(1), 1–13 (2001).
7. Y. C. Liu, K. T. Cheng, Y. D. Chen, and A. Y. Fuh, "All-optically controllable and highly efficient scattering mode light modulator based on azobenzene liquid crystals and poly(N-vinylcarbazole) films," *Opt. Express* **21**(15), 18492–18500 (2013).
8. K. M. Lee, H. Koerner, R. A. Vaia, T. J. Bunning, and T. J. White, "Light-activated shape memory of glassy, azobenzene liquid crystalline polymer networks," *Soft Matter* **7**(9), 4318–4324 (2011).
9. A. Shishido, "Rewritable holograms based on azobenzene-containing liquid-crystalline polymers," *Polym. J.* **42**(7), 525–533 (2010).
10. Y. Yu, M. Nakano, and T. Ikeda, "Photomechanics: directed bending of a polymer film by light," *Nature* **425**(6954), 145–148 (2003).
11. T. J. Bunning, L. V. Natarajan, R. L. Sutherland, and V. P. Tondiglia, "Holographic polymer-dispersed liquid crystals (H-PDLCs)," *Annu. Rev. Mater. Sci.* **30**(1), 83–115 (2000).
12. A. Urbas, J. Klosterman, V. Tondiglia, L. Natarajan, R. Sutherland, O. Tsutsumi, T. Ikeda, and T. Bunning, "Optically switchable Bragg reflectors," *Adv. Mater.* **16**(16), 1453–1456 (2004).

13. L. De Sio, N. Tabiryan, T. Bunning, B. R. Kimball, and C. Umeton, "Dynamic photonic materials based on liquid crystals," *Prog. Opt.* **58**, 1–64 (2013).
14. L. De Sio and N. Tabiryan, "Self-aligning liquid crystals in polymer composite systems," *J. Polym. Sci. Part B Polym. Phys.* **52**(3), 158–162 (2014).
15. E. Ouskova, L. De Sio, R. Vergara, T. J. White, N. Tabiryan, and T. J. Bunning, "Ultra-fast solid state electro-optical modulator based on liquid crystal polymer and liquid crystal composites," *Appl. Phys. Lett.* **105**(23), 231122 (2014).
16. Y. Inoue, H. Yoshida, H. Kubo, and M. Ozaki, "Deformation-free, microsecond electro-optic tuning of liquid crystals," *Advanced Optical Materials* **1**(3), 256–263 (2013).
17. R. A. Vaia, D. W. Tomlin, M. D. Schulte, and T. J. Bunning, "Two-phase nanoscale morphology of polymer/LC composites," *Polymer (Guildf.)* **42**(3), 1055–1065 (2001).
18. A. Rodger, "Circular Dichroism and Linear Dichroism," in *Encyclopedia of Analytical Chemistry* (John Wiley & Sons, Ltd, 2006).
19. U. A. Hrozyk, S. V. Serak, N. V. Tabiryan, L. Hoke, D. M. Steeves, B. Kimball, and G. Kedziora, "Systematic study of absorption spectra of donor–acceptor azobenzene mesogenic structures," *Mol. Cryst. Liq. Cryst. (Phila. Pa.)* **489**, 257–272 (2008).
20. E. Ouskova, A. Pshenychnyi, A. Sanchez-Ferrer, D. Lysenko, J. Vapaavuori, and M. Kaivola, "Enhanced nonlinearity by H-bonded polymer-dye complex in liquid crystal for holographic gratings," *JOSA B* **31**(7), 1456–1464 (2014).
21. D. Statman and I. Janossy, "Study of photoisomerization of azo dyes in liquid crystals," *J. Chem. Phys.* **118**(7), 3222–3232 (2003).
22. F. Simoni, L. Lucchetti, D. Lucchetta, and O. Francescangeli, "On the origin of the huge nonlinear response of dye-doped liquid crystals," *Opt. Express* **9**(2), 85–90 (2001).
23. P. S. Drazic, *Liquid Crystal Dispersions* (World Scientific, 1995).
24. U. A. Hrozyk, S. V. Serak, N. V. Tabiryan, L. Hoke, D. M. Steeves, and B. R. Kimball, "Azobenzene liquid crystalline materials for efficient optical switching with pulsed and/or continuous wave laser beams," *Opt. Express* **18**(8), 8697–8704 (2010).

1. Introduction

Photosensitive materials have been extensively studied in the last few years due to their ability to change mechanical, electrical and optical properties under the influence of light [1–3]. Photosensitive liquid crystals (photo-LCs) are particularly interesting for low-power all-optical switching [4–6], optical phase modulation [7], and optical storage [8, 9]. Photo-LCs are mesogenic photochromic molecules that undergo a reversible *trans-cis* photoisomerization process resulting in strong changes of the optical properties of the material [10]. This transition can be induced with UV/visible light and reversed by heating or longer wavelength irradiation. LC-based photosensitive optical devices are typically sensitive to a molecular director orientation and its confinement topology. Typically, the confinement, stabilization and alignment of photo-LC materials have been studied previously by combining them with isotropic (non-mesogenic) polymeric materials. Diffraction gratings based on photo-LC composite materials such as holographic polymer-dispersed LCs (HPDLCs) [11,12] and polymer liquid crystal polymer slices (POLICRYPS) [13, 14] have been demonstrated. Recently, we demonstrated an ultra-fast solid state phase modulator based on a mesogenic liquid crystal polymer systems [15]. By dispersing a low molar mass LC in a room-temperature mesogenic polymeric matrix, LCPDLC films exhibiting excellent optical and electro-optical phase modulating properties with negligible scattering losses in both the ON and OFF states were demonstrated. The major difference between this system and conventional PDLC systems is that the monomer (and thus polymer) is mesogenic. Compared to other studied systems where the starting LC monomer is a solid [16], our monomer is LC at room temperature enabling easy mixing. This completely changes the starting compatibility of the two major components and greatly affects the phase separation process. The end result is a thin film 'nanocomposite' with small irregularly shaped inclusions of LC which are phase separated from a mesogenic matrix. Advantages to this system include the ability to induce alignment in both the low molar mass LC and the mesogenic monomer (before polymerization), fabrication of complex curved shapes due to the 'liquid' nature of the precursor, and better index matching of the two phases (enabling truly transparent nanocomposites). These are highly promising for applications in systems where fast phase

modulation of an optical signal is needed. Compared to classic PDLC phase retarder systems, the system demonstrated here enables macroscopic polarization control due to alignment control of the polymerized film. Compared to classic 'bulk' LC retarders, the system enables the formation of free standing solid films of any shape which exhibit much faster switching due to small inclusion size of the phase separated LC. We demonstrate here that a LCPDLC system possessing a low molar mass photosensitive LC can be utilized as a scattering-free optically controlled phase modulator.

2. Material and experiments

The LCPDLC film was prepared by mixing an acrylate-based room temperature polymerizable liquid crystalline monomer PLC-2014C (BEAM Co) with 2 wt.% photoinitiator (Darocur-4265, Ciba) and photo-LC. The photo-LC consists of the mesogenic azo dye mixture CPND-57 (BEAMCo), an eutectic composition of two components (homologs): 1-(2-chloro-4-N-n-pentylpiperazinylphenyl)-2-(4-nitrophenyl)diazene (CPND-5) and 1-(2-chloro-4-N-n-heptylpiperazinylphenyl)-2-(4-nitrophenyl)diazene (CPND-7) in the molar ratio 1: 3 dissolved in Nematic LC (NLC) E7 (Merck) at a concentration of 20 wt.%.

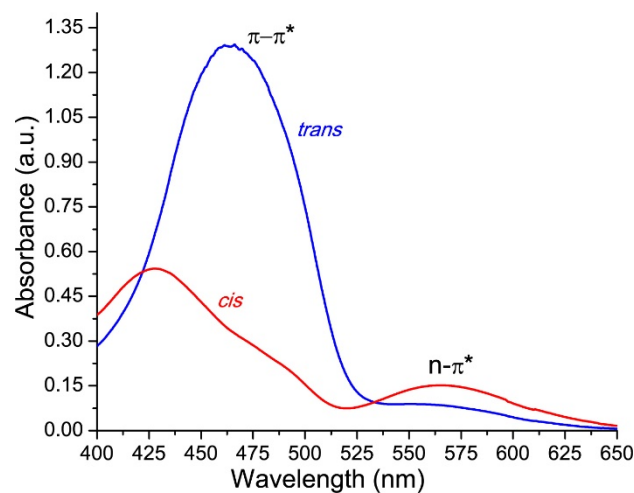


Fig. 1. Visible spectrum of CPND-57 azo-dye dissolved in THF before (blue curve) and after (red curve) irradiation with an external pump beam ($\lambda = 532\text{nm}$).

In Fig. 1 the absorption spectra of the pure CPND-57 azo-dye dissolved in tetrahydrofuran (THF) are reported. In order to characterize the photosensitivity of the solution, we have performed a pump-probe experiment; we have acquired the absorption spectrum after irradiating the sample with a laser source ($\lambda = 532\text{nm}$; $P_{\text{pump}} = 65\text{mW/cm}^2$). CPND-57 exhibits (pump beam off) a strong π - π absorption ($\lambda_{\text{max}} = 460\text{nm}$, blue curve) related to absorption of *trans* isomers, and a lower intensity red-shifted n - π^* absorption band ($\lambda_{\text{max}} = 570\text{nm}$, red curve) due to absorption of *cis* isomers (pump beam on). PLC-2014C was mixed with the photo-LC in a 20/80 ratio by weight. Glass substrates (without ITO) were treated with a polyimide layer and rubbed for a planar orientation. A glass cell with a $9.8\ \mu\text{m}$ gap was filled with the photosensitive LCPDLC mixture by capillary action in darkness above the clearing temperature ($85\ \text{°C}$) ensuring the complete transition to the isotropic state of the LCPDLC composition. Samples were slowly cooled ($2\ \text{K/min}$) to room temperature before photopolymerization ($20\ \text{min}$, $3\ \text{mW/cm}^2$ at $420\ \text{nm}$). Slow cooling is required in order to improve the alignment of the LCPDLC composition. The quality of the alignment for planar LC orientation can be determined by using the aligning quality parameter:

$$\alpha = \frac{I_{\parallel} - I_{\perp}}{I_{\parallel} + I_{\perp}}$$

where I_{\parallel} and I_{\perp} are the intensities of a probe monochromatic light source impinging on the sample placed between crossed (I_{\perp}) and parallel (I_{\parallel}) polarizers, with the LC molecular director oriented parallel to first polarizer. A value of $\alpha = 1$ corresponds to a LC sample that is perfectly unidirectionally aligned, while $\alpha = 0$ corresponds to a LC sample macroscopically randomly aligned (in the plane). We measured $\alpha = 0.996$ (at $\lambda = 633$ nm) indicating an almost perfect alignment of the LCPDLC sample.

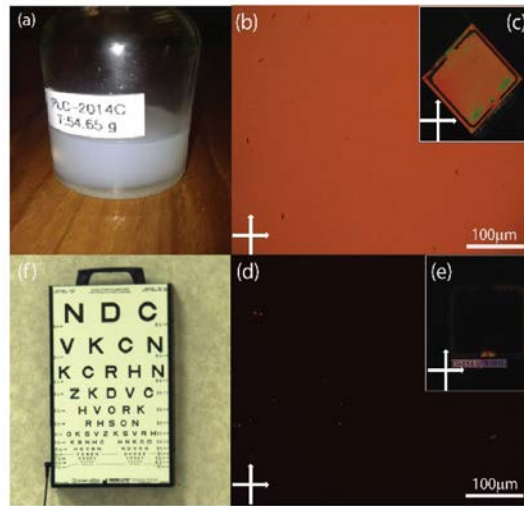


Fig. 2. Photo of the polymerizable liquid crystalline monomer PLC-2014C (a). A photosensitive LCPDLC cell under a microscope with the molecular orientation director (optical axis) making a 45 degree angle with respect to the crossed polarizer/analyzer axes (b). The cell arrangement is shown as an insert (c). The cell is along the polarizer axis in (d) and (e). (f) An eye chart viewed through a photo-LCPDLC at 6m distance (the image was acquired with unpolarized light).

Figure 2(a) is a photo of the polymerizable liquid crystalline monomer PLC-2014C while Figs. 2(b)-2(d) show the polarized optical microscope (POM) view of the LCPDLC sample. The optical contrast between the high and low transmission states of the system between crossed polarizers comprising the LCPDLC cell [Figs. 2(b)-2(d)] is better than 60:1 for white noncollimated light. Photos of the cell obtained between crossed polarizers at 45° and 0° angle of the molecular orientation axis of LCPDLC with respect to the axis of the polarizer confirm uniform alignment of the material across the cell, [Figs. 2(c)-2(e)]. In order to show that the LCPDLC does not scatter visible radiation, an image of an eye chart was taken through the sample with a high resolution camera at a distance of 6m. The image shown in Fig. 2(f) has a slight orange tint due to absorption of the LC material itself but, the 20/20 line is visible indicating the absence of light scattering due to structural inhomogeneity or large-scale two-phase microstructures. The interior sample morphology was analyzed in detail with low voltage (1 keV) high-resolution scanning electron microscopy (HRSEM) (details on the technique are reported in [17]) and with bright-field transmission electron microscopy (BFTEM). The sample was fractured in liquid nitrogen and coated with 3 nm of tungsten for SEM analysis and was embedded in EPOX 812, microtomed into 75 nm thick films, and stained with RuO₄ for 1 hr before imaging at 200kV.

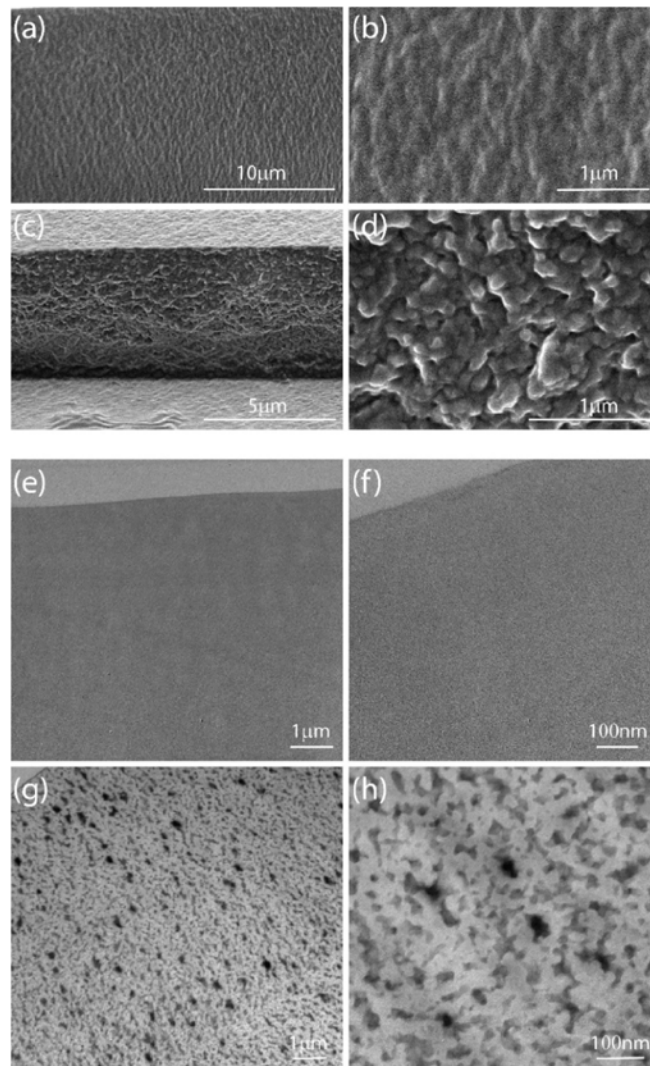


Fig. 3. High resolution scanning electron microscope (a, b, c, d) and bright-field transmission electron microscopy (e, f, g, h) analysis of the sample. The sample has been analyzed without (a, b, e, f) and with (c, d, g, h) the presence of photo-LC.

Figure 3 shows HRSEM/BFTEM images at several scales for the sample containing low molar mass LC [Figs. 3(c)-3(d)-3(g)-3(h)] and as a control the morphology of the sample polymerized without LC [Figs. 3(a)-3(b)-3(e)-3(f)]. The BFTEM images [Figs. 3(g)-3(h)] clearly indicate a two phase morphology as small irregular shaped dark inclusions reside in a matrix of lighter electron density. In fact the photo-LC, driven in part by the slow photo-initiated polymerization kinetics, “escapes” from the growing polymeric matrix and collect in trapped regions. The final phase morphology resulting from this process of phase separation is a co-continuous two phase morphology where both PLC and photo-LC phases coexist. The average size of the photo-LC domains is sub 100nm, consistent with the lack of optical scatter from the sample. In comparison, little structure is present in films fabricated from the sample without LC [Figs. 3(a)-3(b)-3(e)-3(f)]. This comparison clearly demonstrates the nano-structured two phase interior morphology present. The HRSEM images [Figs. 3(c)-3(d)] confirm this as a fracture surface with irregular topography possessing similar length scale is observed. The HRSEM images also reveal non-spherical polymerized inclusions consistent

with preferential alignment imposed by the rubbed glass substrates on the monomer fluid and then polymerization.

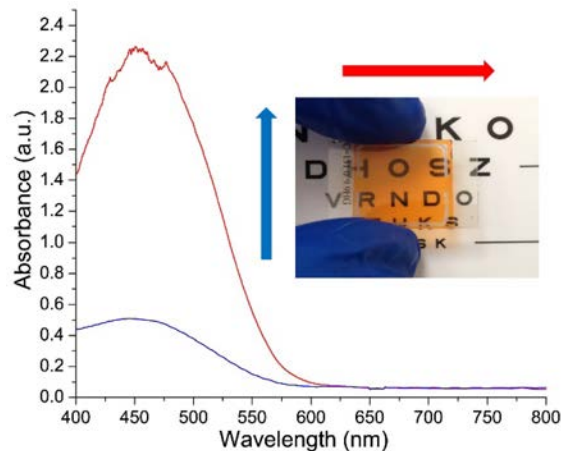


Fig. 4. Polarized spectral response for two orthogonal impinging polarizations. The red and blue curves have been acquired for light polarized along (red arrow, inset) and perpendicular (blue arrow, inset) the alignment direction. In the inset there is a photo of the sample.

The spectral response of the sample (Fig. 4) shows an absorption peak centered at 465 nm with a strong correlation between the amplitude of the absorption peak (red and blue curve) and the polarization direction of incident light. Strong linear dichroism is evident ($LD \sim 1.8$ abs.u.), as defined [18] as the difference between the amplitude of the absorption peak obtained for light polarized parallel (red arrow, inset of Fig. 4) and perpendicular (blue arrow, inset of Fig. 4) to the orientation axis $LD = A_{\parallel} - A_{\perp}$. This suggests that the LCPDLC molecules are very well aligned along the rubbing direction. The corresponding order parameter, $S = (A_{\parallel} - A_{\perp}) / (A_{\parallel} + 2A_{\perp})$ is about 0.55, typical for azo-benzene type LCs.

3. Results

The optical setup utilized for sample characterization [Fig. 5(c)] makes use of a green pump laser emitting at 532 nm and a He-Ne probe beam of 633 nm wavelength. The sample is placed between crossed polarizers with the optical axis at 45° to the polarizer/analyzer axes. The dynamics of transmission variation of the light sensitive LCPDLC [Fig. 5(a)] is monitored by a photodetector for different values of the pump power density varied from 3 mW/cm^2 to 31 mW/cm^2 while the probe power density (0.05 W/cm^2) is kept constant. Figure 5(a) clearly shows the strong correlation between the variation of the transmitted intensity and the external pump power. The pump beam induces *trans-cis* photoisomerization, reducing the photo-LC order in the phase separated regions, thereby decreasing the transmission of the system between crossed polarizers. At the steady state with the pump beam on, we have observed a slow drift of the curves particularly for the $P_{\text{pump}} = 31 \text{ mW/cm}^2$ case [Fig. 5(a), red curve]. This behavior can be explained by considering that for longer illumination times there is a competition between photo-induced *trans-cis* isomerization and the spontaneous relaxation (*cis-trans*). However, the aforementioned competition does not affect the response times of the sample. The transmitted intensity is restored to its initial value [Fig. 5(a)] due to spontaneous *cis-trans* relaxation upon turning off the laser beam. The different relaxation times from *cis* to *trans* isomers are due to the fact that the relaxation time from *cis* to *trans* is proportional to the rate of concentration of photoisomerized molecules which in turn is proportional to the incident intensity. Noteworthy, the initial transmission values [Fig. 5(a)] are slightly different because when the pump beam is turned off at the end of the first

measurement, the transmitted intensity is not fully restored to the same initial value. Thus, when the power for performing the new transmission dynamic experiment is increased, the new curve starts from a slightly different value. This phenomenon can be avoided by waiting longer waiting times between two consecutive measurements to fully enable complete relaxation. However, since our goal was to measure the response time vs the impinging power density, we performed the experiments every 40 seconds [Fig. 5(a)]. The switching times (τ_{sw}) as a function of pump power obtained from the analysis of the curves is shown in Fig. 5(b). The data are well fitted by an exponential decay curve [Fig. 5(b), blue curve]:

$$\tau_{sw} = \tau_0 e^{-(P-P_{min})/P_0}$$

where $\tau_0 = 10.9$ s and $P_0 = 11.34$ mW. P is the impinging pump power while P_{min} is the minimum power below which the effect is very small and it is almost impossible to get a good signal. This behavior is explained by assuming the ratio of concentration of photoisomerized molecules (*trans-cis*) is proportional to the incident intensity [19]. As reported in [20], the order parameter S of a LC doped mixture (in our case PLC doped with photo-LC) depends on the concentration of the transformed molecules (*trans-cis*) of the dopant (photo-LC, in our case). By increasing the pump intensity, the amount of the *cis* isomer molecules grows by affecting (reducing) S . As a consequence, the higher the intensity, the lower S becomes with a consequent reduction of the switching time [21].

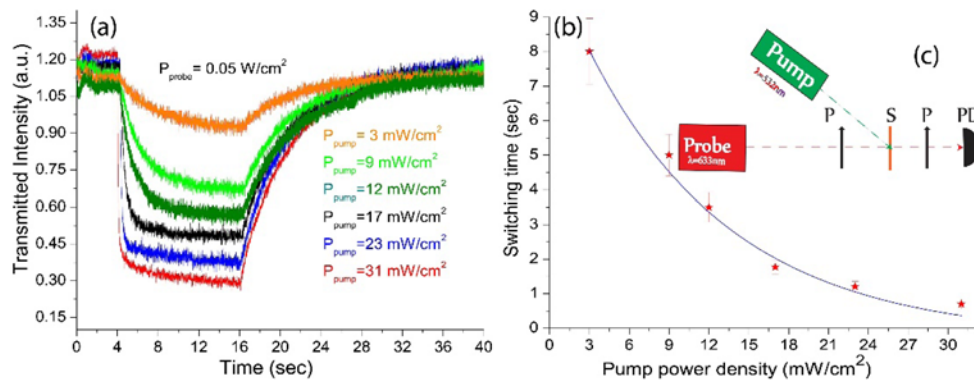


Fig. 5. (a) Transmission dynamics and (b) response time of photo-LCPDLC sample as a function of pump power density. Sketch of the experimental setup (c) used in the test. P, polarizer; S, sample, PD, photo-detector.

It is worth pointing out that the correlation between the variation of the transmitted intensity and the external pump power reported in [Fig. 5(a)] cannot be associated to the anisotropic reorientation of photo-LC (the so called optical Freedericksz transition). This effect can be induced by means of typical optical power of the order of 0.3-0.5 W/cm² [22]. In our case, we use a pump power of the order of 0.031 W/cm² which is much lower than the minimum threshold (0.3 W/cm²) for inducing optical reorientation in the presence of photo-LC. In addition, when the optical Freedericksz transition is present, the typical response times are of the order of 100-200 seconds. In our case, the response times (few seconds) are much faster suggesting the effect is due to *trans-cis* photo-isomerization process. The switching was found to be repeatable and reversible [Fig. 6(a)] using a periodic sequence of pump beam pulses. Finally, optically induced birefringence variations were characterized by measuring transmission spectra between parallel polarizers with the optical axis of the cell at 45° to the polarizer/analyzer axes. Changes in the transmission spectrum for a white light source at normal incidence were registered upon the influence of the pump beam [Fig. 6(b)]. Both the amplitude and the position of the peak in the spectra decrease with increasing pump power

density. The reduction in transmitted intensity [Fig. 6(b)] is correlated to a decrease in transmission of the sample under the pump beam illumination which is related to the scattering of the impinging radiation due to a slight refractive index mismatch between the PLC and photo-LC domains. The spectra in Fig. 6(b) can be used for evaluating the absolute value of the birefringence (Δn) and its variation under the influence of the optical field. The maxima in the transmission spectra fulfil the condition $\Delta n \cdot d = m \cdot \lambda$ [23] where d is the cell thickness, m is an integer ($m = 1$, in our case) and λ is the wavelength. The birefringence of the material was evaluated to be $\Delta n = 0.13$ in the absence of the pump beam and it was reduced to 0.12 for $P = 31 \text{ mW/cm}^2$. The corresponding phase range of the LCPDLC film was estimated to be equal to $\pi/3$ (for $0.532 \text{ }\mu\text{m}$ wavelength).

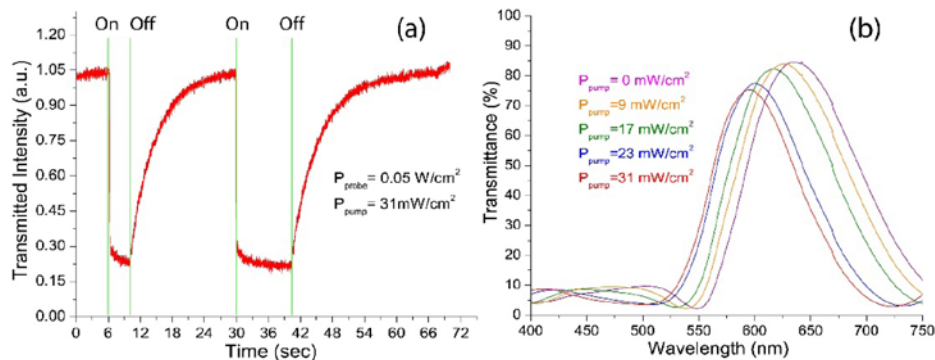


Fig. 6. (a) Cycling photo-LCPDLC between high and low transmission states. ON and OFF refer to unblocking and blocking the pump beam. (b) Transmission spectra between parallel polarizers for different values of pump power density.

The residual birefringence $\Delta n = 0.12$ is due to the well oriented PLC; indeed, PLC, after the polymerization process, does not change its properties (e.g. birefringence) under the influence of the pump beam.

4. Conclusions

We have demonstrated a photo addressable liquid crystal polymer-dispersed liquid crystal (LCPDLC) system. Both polarized optical microscopy and high resolution electron microscopy confirm a distinct nanoscale two-phase morphology. Bright field transmission electron microscopy shows a two-phase morphology with small irregular shaped dark inclusions ($<100 \text{ nm}$) within a matrix of lighter electron density material. These films exhibit good transparency enabling imaging without distortion and haziness. The photosensitive properties of the LCPDLC characterized by a pump-probe setup are promising for controlling the transmitted light intensity (through crossed polarizers) and phase with a relatively low pump beam power density. Compared to classic PDLC phase retarder systems, LCPDLC is completely clear in the off state (pump beam off) and it exhibits very low scattering losses in the on state (pump beam on). Moreover, since we use all mesogenic materials (PLC, NLC and azo-dye), we can easily play with the concentrations in order to maximize the phase change. The response times of the LCPDLC system can be improved by optimizing the materials or using a pulsed pump beam. In fact, the photo-induced *trans-cis* isomerization process can be speed up using a pulsed pump beam [24] for the following mechanisms: (i) the excitation of a pulsed pump beam concentrates the required energy density in a short time interval (ns range); (ii) since the material (azo-dye) possesses a very short spontaneous relaxation time (ms), the response time is due to the balance between the *trans-cis* isomerization process (ns process) and the spontaneous relaxation of the material (*cis-trans*). By using a pulsed beam (e.g. ns pulse) the spontaneous relaxation of the material does not affect the process because is several order of magnitude slower.